Time-Resolved Infrared Spectroscopy of Intermediates and Products from Photolysis of 1-(2-Nitrophenyl)ethyl Phosphates: Reaction of the 2-Nitrosoacetophenone Byproduct with Thiols

Andreas Barth,[†] John E. T. Corrie,*[,‡] Michael J. Gradwell,[‡] Yashusi Maeda,[†] Werner Mäntele,[†] Tanja Meier,[†] and David R. Trentham[‡]

Contribution from the Institut für Theoretische und Physikalische Chemie, Universität Erlangen, Egerlandstrasse 3, 91058 Erlangen, Germany, and National Institute for Medical Research, The Ridgeway, Mill Hill, London NW7 1AA, UK

Received December 27, 1996[⊗]

Abstract: Rapid scan Fourier transform infrared (FTIR) spectroscopy and time-resolved single wavelength infrared (IR) spectroscopy have been applied to study the mechanism of photochemical release of adenosine 5′-triphosphate (ATP) from its P^3-[1-(2-nitrophenyl)ethyl] ester (caged ATP). Bands arising from phosphate and non-phosphate vibrations characteristic of the *aci*-nitro anion intermediate and from free ATP and byproducts of the nitrophenylethyl group have been assigned using ^{13}C, ^{15}N, and ^{18}O isotopomers of caged ATP. Monitoring several of these bands using time-resolved single frequency IR spectroscopy confirms that release of ATP occurs in a single exponential process synchronous with the decay of the *aci*-nitro anion intermediate. Spectral characteristics of the reaction products arising from the 1-(2-nitrophenyl)ethyl group in the absence and presence of dithiothreitol (DTT) have been determined. The major final byproduct from photolysis conducted in the presence of DTT is 3-methylanthranil. The mechanism of formation of this compound from 2-nitrosoacetophenone has been investigated in detail by a combination of spectroscopic, kinetic, and chemical methods and reconciled with earlier data. The byproduct species likely to be present on the time scale of most biological experiments using caged compounds is 2-hydroxylaminoacetophenone as a mixture of ring-chain tautomers.

Introduction

Over the last decade flash photolysis of photolabile but biologically inert molecules ("caged" compounds) to release biological effectors has had significant impact on the analysis of rapid physiological processes. By their nature such processes demand kinetic analysis, and the rate and mechanism of the photorelease are an integral part of this. Therefore it is desirable to have a direct, noninferential method for measurement of photorelease rates from caged compounds. We recently described the use of rapid scan Fourier transform infrared (FTIR) spectroscopy and time-resolved single wavelength infrared spectroscopy to determine the rate of ATP release upon photolysis of caged ATP, the P^3-[1-(2-nitrophenyl)ethyl] ester of adenosine triphosphate **1a**.[1] The spectroscopic data in the earlier paper were principally concerned with interpretation of changes in phosphate vibrational modes among the starting material **1a**, the intermediate *aci*-nitro anion **2**, and the final free ATP (see Scheme 1). The ^{18}O isotopomers **1b** and **1c** were used to help make secure assignments of phosphate-associated bands in the intermediate **2** and the ATP end product. Based on these assignments, time-resolved single wavelength IR spectroscopy enabled direct measurement of the rate of free ATP formation. Several matters remained unanswered, including a lack of specific assignments for non-phosphate vibrational bands associated with the *aci*-nitro intermediate **2**. In addition we had been unable to make definitive assignments of particular phosphate bands, especially in the region near 1260 cm^{-1}, and there was a discrepancy between the rate of ATP formation

Scheme 1

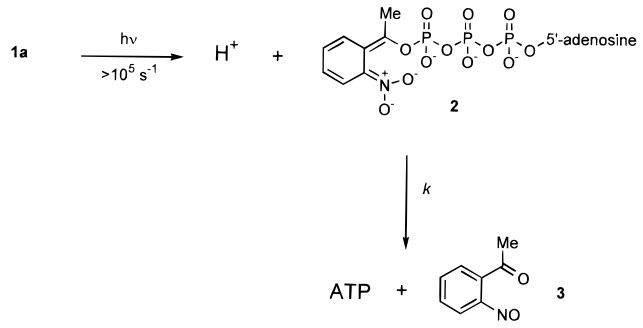

measured by IR and that expected from previous measurements[2,3] that were based on transient UV spectroscopy of the *aci*-nitro chromophore.

The present paper gives near-complete band assignments through the use of further isotopomers of caged ATP which contain ^{15}N in the nitro group (**1d**) or ^{13}C in the benzylic carbon (**1e**), together with corresponding isotopomers of caged methyl phosphate **4a** and the [$\beta,\beta\gamma$-$^{18}O_3$]caged ATP isotopomer **5**. Spectra of caged methyl phosphate are not described in detail but are used to clarify particular assignments. Discrepancies in the rates of ATP formation measured by different techniques have been resolved and rationalized by a combination of transient UV spectroscopy of solutions of caged ATP photolyzed under the conditions of the IR measurements, together with consideration of the pH of solutions used for measurements. We have also used IR spectroscopy to aid identification of

* Author to whom correspondence should be sent.
† Universität Erlangen.
‡ National Institute for Medical Research.
⊗ Abstract published in *Advance ACS Abstracts,* April 15, 1997.
(1) Barth, A.; Hauser, K.; Mäntele, W.; Corrie, J. E. T.; Trentham, D. R. *J. Am. Chem. Soc.* **1995**, *117*, 10311−10316.
(2) Walker, J. W.; Reid, G. P.; McCray, J. A.; Trentham, D. R. *J. Am. Chem. Soc.* **1988**, *110*, 7170−7177.
(3) McCray, J. A.; Trentham, D. R. *Annu. Rev. Biophys. Biophys. Chem.* **1989**, *18*, 239−270.

S0002-7863(96)04430-7 CCC: $14.00

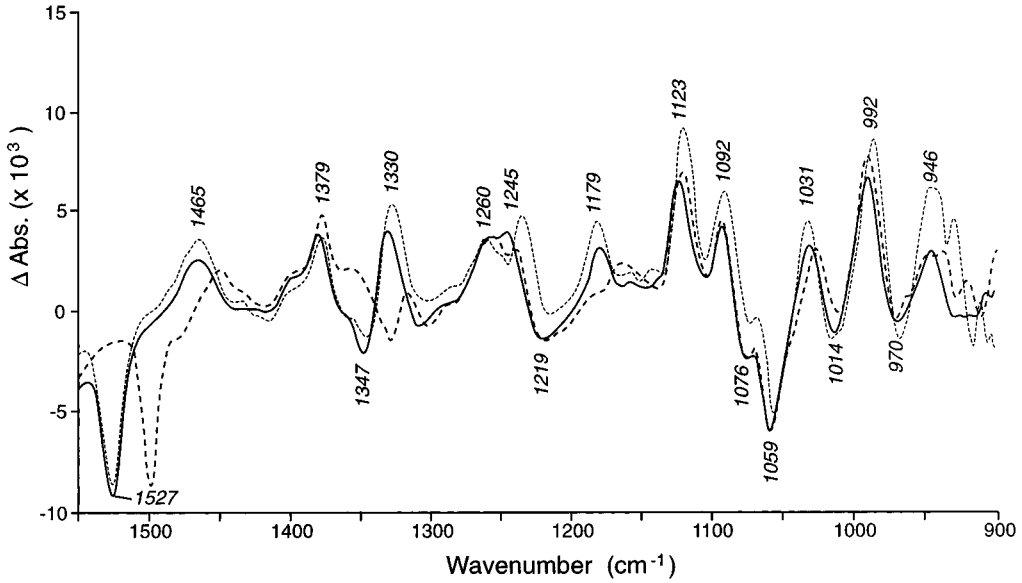

Figure 1. Infrared difference spectra of caged ATP photolysis at pH 8.5, 1 °C recorded 4-60 ms after the photolysis flash. Solid line, compound **1a**; dashed line, compound **1d**; dotted line, compound **1e**. Labels refer to peaks in the solid line spectrum.

byproducts which arise from the cage group after photolysis and especially to unravel the multistep process which occurs when photolysis is performed in the presence of a thiol. Thiols have been used since the first descriptions of caged compounds in biology[4] to remove 2-nitrosoacetophenone **3** formed as the initial byproduct (Scheme 1), but the underlying chemistry had not been defined. Since byproducts are likely to be formed in millimolar concentrations in parallel with release of the biological effector species, it is desirable to have information about their nature.

Results and Discussion

The IR difference spectra shown in the figures follow the same convention as previously,[1] i.e., negative bands are associated with absorption by the starting caged compound and positive bands represent absorption by the species present at the time of acquisition of the spectrum. Difference spectra of Figures 1 and 2 were acquired at pH 8.5 and 1 °C as described previously.[1] The unphotolyzed caged compound served as the reference spectrum, and spectra recorded in the first 60 ms after the photolysis flash represent almost entirely the transition from caged compound to the *aci*-nitro intermediate **2**, whereas spectra accumulated from 2.7 to 23 s after photolysis represent >99% of the transition from caged to free ATP. As discussed below and depending upon the experimental conditions, chemistry involving the byproducts may not be complete until more time has elapsed.

Transition of Caged ATP to the *aci*-Nitro Intermediate. Figure 1 shows difference spectra in the range 900−1550 cm^{-1} for the absorption of the *aci*-nitro anion **2** and relevant isotopomers minus absorption of starting material for caged ATP **1a** and isotopomers **1d** and **1e**. Figure 2a shows corresponding *aci*-nitro anion spectra for **1a** and the $\beta,\beta\gamma$-$^{18}O_3$ isotopomer **5**. Related spectra for the γ-^{18}O isotopomers **1b** and **1c** were reported previously.[1]

(a) ^{15}N Isotopomer. For the ^{15}N isotopomer **1d**, large spectral shifts arising from the isotopic substitution are only observed in the region above 1160 cm^{-1}. As expected, the negative bands at 1527 and 1347 cm^{-1} from the antisymmetric and symmetric NO_2 vibrations of caged ATP are strongly downshifted by 28 and 17 cm^{-1} respectively. The negative band from the symmetric [^{15}N]nitro vibration overlaps with a positive band at 1318 cm^{-1}, and its true position is probably nearer to 1325 cm^{-1} where it appears without overlap in the spectrum recorded after 2.7 s (data not shown). The true downshift is therefore ∼22 cm^{-1}, consistent with the reported shift of 24 cm^{-1} for the ν_s vibration of [^{15}N]nitrobenzene.[5] Three positive bands at 1465, 1330, and 1179 cm^{-1} are downshifted 12−15 cm^{-1} by ^{15}N substitution to 1451, 1318, and 1164 cm^{-1}, respectively. Similar bands and shifts are observed for the *aci*-nitro intermediate from caged methyl phosphate **4a** and its ^{15}N

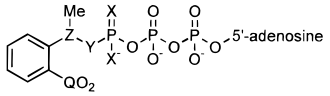

1a Q = ^{14}N, Z = ^{12}C, X,Y = ^{16}O
1b Q = ^{14}N, Z = ^{12}C, X = ^{16}O, Y = ^{18}O
1c Q = ^{14}N, Z = ^{12}C, X,Y = ^{18}O
1d Q = ^{15}N, Z = ^{12}C, X,Y = ^{16}O
1e Q = ^{14}N, Z = ^{13}C, X,Y = ^{16}O

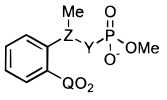

4a Q = ^{14}N, Y = ^{16}O, Z = ^{12}C
4b Q = ^{15}N, Y = ^{16}O, Z = ^{12}C
4c Q = ^{14}N, Y = ^{16}O, Z = ^{13}C
4d Q = ^{14}N, Y = ^{18}O, Z = ^{12}C

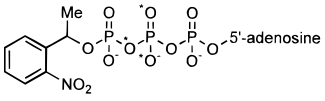

5

isotopomer **4b**. The isotopic shifts of the three bands are smaller than those for the nitro bands of the starting compounds and suggest that the corresponding vibrations are less localized in the *aci*-nitro intermediates. We refer at other points in the text to the high degree of coupling which is apparent among vibrational modes of these intermediates. Proposed assignments are that the 1465 cm^{-1} band corresponds to the stretching vibration of the *aci*-nitro C═N bond, while the 1330 and 1179 cm^{-1} bands derive from antisymmetric and symmetric N−O

(4) Kaplan, J. H.; Forbush, B.; Hoffman, J. F. *Biochemistry* **1978**, *17*, 1929−1935.

(5) Dähne, S.; Stanko, H. *Spectrochim. Acta* **1962**, *18*, 561−567.

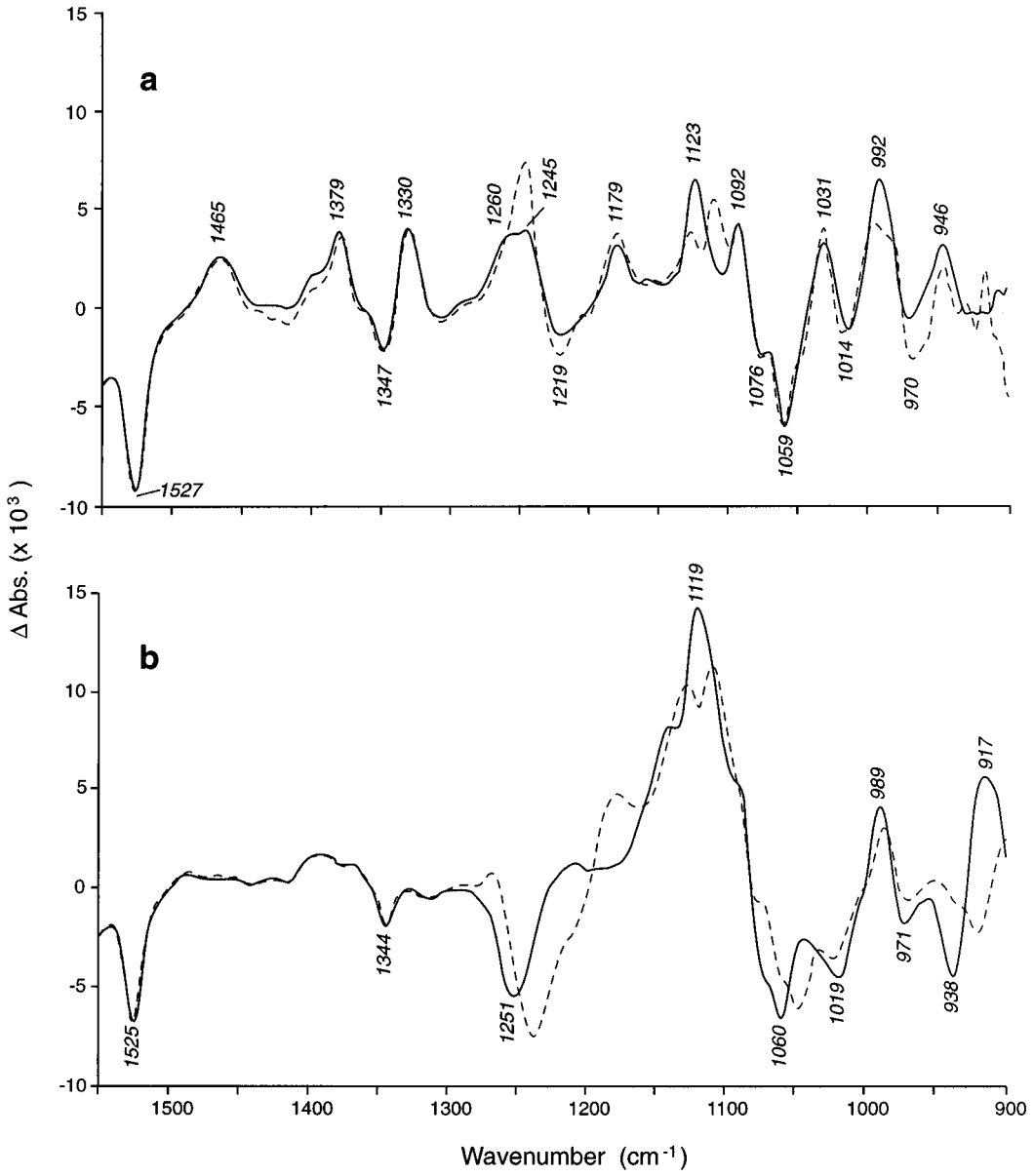

Figure 2. Infrared difference spectra of caged ATP photolysis at pH 8.5, 1 °C. Solid line, compound **1a**; dashed line, compound **5**. (a) Spectra obtained 4−60 ms after the photolysis flash. (b) Spectra obtained 2.7−23 s after the photolysis flash. The labels refer to peaks in the solid line spectrum.

stretching vibrations of the nitronate. The positions of the latter two bands are at the upper end of the range of values given by Feuer *et al.*[6] for alkylnitronate salts, i.e., 1205−1316 and 1040−1175 cm^{-1}, for the antisymmetric and symmetric stretches. The same authors reported the C═N stretching frequency for these nitronates in the range 1587−1605 cm^{-1}, compared to our value of 1465 cm^{-1}. Evidently bond orders in the *aci*-nitro intermediate differ substantially from those indicated by structure **2**, implying that other canonical forms make significant contributions to the resonance hybrid. Small downshifts of 1−3 cm^{-1} are observed for bands that appear in the spectrum deriving from photolysis of the nonisotopic compound **1a** at 1379, 1245, 1123, 1031, and 1014 cm^{-1}. These shifts suggest that the nitrogen atom of the nitro group is involved to a minor extent in the corresponding vibrations.

(b) ^{13}C Isotopomer. The largest effect in the spectrum of the intermediate from ^{13}C isotopomer **1e** is a downshift of the band at 1245 to 1234 cm^{-1}. This band and its adjacent shoulder at 1260 cm^{-1} were subjects of some conjecture in our earlier paper,[1] where it was proposed that the band at 1260 cm^{-1} involved PO_2^- vibrations but the band at 1245 cm^{-1} did not. In the spectrum of the intermediate from caged methyl phosphate **4a**, a comparable band appears at 1244 cm^{-1} (shifted to 1242 cm^{-1} in ^{18}O isotopomer **4d**) and is downshifted to 1233 cm^{-1} in the ^{13}C isotopomer **4c**. The shift observed upon ^{13}C substitution in the benzylic carbon of both caged compounds, together with the lack of a comparable shift upon ^{18}O substitution of the bridging oxygen, indicates that the band involves a carbon−carbon vibration in the C═C(Me)O system of the *aci*-nitro intermediate **2**. A shift of 11 cm^{-1} is smaller than expected (∼25 cm^{-1}) for an isolated C−C oscillator and indicates that other parts of the molecule are also involved, as is supported by the small ^{18}O and ^{15}N shifts described above. The ^{13}C shift also confirms the presence of two separate vibrational modes (1260 and 1245 cm^{-1}) in this region of the spectrum.

The only other substantial isotope effect for the ^{13}C isotopomer is in the positive band at 992 cm^{-1}, which shifts to 985 cm^{-1}. This is consistent with the previous interpretation that

(6) Feuer, H.; Savides, C.; Rao, C. N. R. *Spectrochim. Acta* **1963**, *19*, 431−434.

absorptions in this region are associated with coupled C−O−$(PO_3)_3$−C backbone modes perturbed by formation of the *aci*-nitro intermediate. Small downshifts (2−4 cm^{-1}) are evident for several bands below 1380 cm^{-1}, which again indicates extensive coupling of vibrations involving the benzylic carbon with other vibrational modes. An unassigned positive band at 1379 cm^{-1}, which was hardly affected by ^{15}N substitution, is downshifted by 2 cm^{-1} while the positive 1330 cm^{-1} band, tentatively assigned above to ν_{as} of the $=NO_2^-$ system is downshifted by 4 cm^{-1}. Both bands have the same shifts in spectra from photolysis of [^{13}C]caged methyl phosphate **4c** and must be associated with the *aci*-nitro portion of the intermediate **2**. It appears reasonable in view of the extended conjugation of the *aci*-nitro moiety that there should be small effects of ^{13}C substitution on many of the vibrational modes. More surprising are the respective 4 and 2 cm^{-1} downshifts of the strong positive bands at 1123 and 1092 cm^{-1} and the 2 cm^{-1} downshift of the negative band at 1076 cm^{-1}. We previously[1] assigned these bands to symmetrical PO_2^- modes on the basis of our own ^{18}O results and those of Takeuchi *et al.*,[7] who assigned the highest wavenumber vibration to an in-phase mode and the two lower wavenumber bands to out-of-phase modes. Since the vibrations of the entire triphosphate chain are coupled, the effect of ^{13}C substitution in **1e** could be expected to be felt by all three of the observed symmetrical PO_2^- modes. Similarly the negative band at 1059 cm^{-1}, previously assigned[1] to a ν_s PO_2^- vibration predominantly involving the γ-phosphate, shows a downshift of 4 cm^{-1} with ^{13}C substitution. These small effects on phosphate modes are similar in magnitude to the effects of ^{15}N substitution on the phosphate bands at 1123, 1031, and 1014 cm^{-1} (see above). However it is notable that the shifts caused by the two isotopic substitutions affect different subsets of phosphate modes.

(c) $\beta,\beta\gamma$-$^{18}O_3$ Isotopomer. As expected from our previous results,[1] the spectrum of *aci*-nitro intermediate formation from $\beta,\beta\gamma$-$^{18}O_3$ isotopomer **5** showed no isotopic shifts in the range 1550−1300 cm^{-1} (Figure 2a). In common with the spectrum of *aci*-nitro intermediate formation from γ-isotopomer **1c**, the positive band seen for the unlabeled intermediate at 1260 cm^{-1} is downshifted and overlaps with the vibration at 1245 cm^{-1}, which does not involve the PO_2^- group (see above), to give an intense positive band with a maximum at 1246 cm^{-1} (*cf.* 1242 cm^{-1} for **1c**).[1] Since this 1260 cm^{-1} band is similarly affected by both β- and γ-^{18}O substitution, it is evident that at least some of the ν_{as} PO_2^- modes in the *aci*-nitro intermediate **2** are coupled. The negative band at 1219 cm^{-1} was previously assigned[1] to a ν_{as} PO_2^- vibration of caged ATP to which the γ-phosphate contributes and as expected remains unaffected by β-labeling in compound **5**, while a shoulder at ∼1205 cm^{-1} suggests the presence of a weak positive band. For the γ-labeled compound **1c**, where the negative 1219 cm^{-1} band is downshifted to ∼1180 cm^{-1}, it is notable that a well-resolved positive band is present at 1209 cm^{-1}, while both **1a** and **1b** show an inflection at this point in the profile of the 1219 cm^{-1} negative band.

To summarize this spectral region for the *aci*-nitro intermediate **2**, it appears that the ν_{as} PO_2^- vibration of the γ-phosphate is upshifted in frequency when the *aci*-nitro intermediate forms to give the positive band at 1260 cm^{-1} and the negative band at 1219 cm^{-1}, both of which are sensitive to γ-$^{18}O_3$ substitution. In caged ATP itself this γ-PO_2^- vibration is not coupled to the β-PO_2^- vibrations but does couple in the *aci*-nitro intermediate. The intensity of the absorption around 1260 cm^{-1} is diminished in caged ATP **1a** by an overlapping ν_{as} negative band at 1251 cm^{-1} involving the α- and β-phosphates.[1] When this band is absent as in caged methyl phosphate **4a** or downshifted by β-^{18}O substitution (see below), the absorption intensity in the region 1245−1260 cm^{-1} is substantially enhanced. These ν_{as} PO_2^- bands are overlaid by the C=C(Me)O band at 1245 cm^{-1} as discussed above and by a positive band at 1209 cm^{-1} which probably involves the α-phosphate, since it is unaffected by β- or γ-^{18}O labeling.

The ν_s PO_2^- stretching modes around 1100 cm^{-1} are affected by β-^{18}O substitution. Most notably the intense positive band at 1123 cm^{-1} in the spectrum of the *aci*-nitro intermediate derived from the unlabeled compound **1a** splits into two bands at 1127 and 1110 cm^{-1} in the difference spectrum arising from photolysis of compound **5**. This double peak probably does not represent two different vibrational modes but instead arises from overlap of a negative band near 1120 cm^{-1} with a positive band in the region 1110−1130 cm^{-1}. The negative band can be assigned to a ν_s PO_2^- vibration of caged ATP, seen as a band in the absorbance spectrum (not shown) at 1131 cm^{-1} for **1a** and **1b**, at 1123 cm^{-1} for **1c**, and at 1115 cm^{-1} for **5**. Upon formation of the *aci*-nitro intermediate **2**, the vibration appears to intensify and shift slightly, as indicated by the positive band in the range 1120−1130 cm^{-1} in the difference spectra for isotopomers **1a**−**c** and **5**. Only for **5** do the positive and negative bands overlap in such a way that the difference spectrum shows two separate positive peaks. The mode appears to be more delocalized in the *aci*-nitro intermediate than in caged ATP and to involve vibrations other than pure ν_s PO_2^- modes, since its position is less affected by β- or γ-$^{18}O_3$ substitution than in caged ATP but is sensitive to ^{13}C and ^{15}N substitution. Takeuchi *et al.*[7] suggested that there was extensive mixing of the ν_s PO_2^- vibrations among the three phosphate groups of ATP at pH 3, where protonation of the terminal phosphate simulates the effect of alkylation in caged ATP. Our results indicate that coupling is also possible with groups remote from the triphosphate. Similar effects are observed in the spectrum of *aci*-nitro formation from caged methyl phosphate **4a**, where the band at 1126 cm^{-1} shows downshifts of 3 cm^{-1} for ^{15}N substitution (**4b**), 4 cm^{-1} for ^{13}C substitution (**4c**), and 2 cm^{-1} for $^{18}O_1$ substitution (**4d**).

The positions of the positive band at 1092 cm^{-1} and negative bands at 1076 and 1059 cm^{-1} are essentially unaffected in **5**, although a small new shoulder appears at 1047 cm^{-1}. These bands were previously[1] assigned to ν_s PO_2^- modes following Takeuchi *et al.*[7] and because they were shifted upon γ-$^{18}O_3$ substitution. The lack of a significant isotope effect upon β-$^{18}O_3$ substitution shows that the ν_s vibrations of the β-PO_2^- group do not contribute.

The positive band at 1031 cm^{-1}, which is downshifted to 1020 cm^{-1} in the γ-$^{18}O_3$ isotopomer **1c**, is unaffected in the $\beta,\beta\gamma$-$^{18}O_3$ isotopomer **5** but the remaining band profile below 1020 cm^{-1} is characterized by splitting of the sharp bands at 1014 (negative), 992 (positive), and 970 cm^{-1} (negative) to give broadened bands at 1019/1014, 995/984, and 967/957 cm^{-1}, respectively. This pattern is more complex than the generalized downshift that was observed for the γ-$^{18}O_3$ isotopomer **1c** but is in line with the previous assignment to delocalized C−O−$(PO_3)_3$−C backbone modes.[1]

The information gained from isotopomers **1d**, **1e**, and **5** is consistent with the previous interpretation[1] of the difference spectra for formation of the *aci*-nitro intermediate **2**. In particular the band at 1245 cm^{-1}, which contributed intensity to the previous[1] single wavelength kinetic monitoring at 1251

(7) Takeuchi, H.; Murata, H.; Harada, I. *J. Am. Chem. Soc.* **1988**, *110*, 392−397.

cm^{-1}, has been shown to involve a vibrational mode associated with the *aci*-nitro portion of the intermediate **2**.

Overall Transition from Caged To Free ATP at pH 8.5 in the Absence of a Thiol. This section is principally concerned with analysis of changes in phosphate modes when ATP is released from the *aci*-nitro intermediate **2**. Experiments under different conditions have enabled characterization of the byproducts arising from the 1-(2-nitrophenyl)ethyl group and are described in later sections. Figure 2b shows difference spectra of the photolyzed solution accumulated in the time range 2.7−23 s after the photolysis flash for caged ATP **1a** and its $\beta,\beta\gamma$-$^{18}O_3$ isotopomer **5**. Corresponding spectra for the γ-^{18}O isotopomers **1b** and **1c** have been published previously.[1] End spectra for the ^{15}N and ^{13}C isotopomers **1d** and **1e** are not shown, since with a few exceptions there were only very minor perturbations of weak bands in the region 1800−1250 cm^{-1}. The exceptions include the large shifts for the negative bands arising from the nitro group in **1d** already described above. Changes in the intensity and position of the nitro bands during the transition from the *aci*-nitro intermediate to ATP and byproducts are discussed in the following section on single wavelength kinetic measurements. The remaining exceptions are a shift of the carbonyl absorption of the 2-nitrosoacetophenone byproduct for the ^{13}C compound **1e** (see below) and a weak positive band at 1265 cm^{-1} which is evident in the end spectrum of photolysis of caged methyl phosphate **4a** and shifts to 1249 cm^{-1} with ^{13}C substitution. This band is also present in the caged ATP spectra but is obscured by the large negative band at 1251 cm^{-1}. However it is visible at 1268 cm^{-1} in the spectrum of the $\beta,\beta\gamma$-$^{18}O_3$ isotopomer **5** because of the downshift of the negative band (see below). The magnitude of the ^{13}C-induced shift is compatible with a localized C−C vibration and a reasonable assignment is to the Ar−C bond of the byproduct **3**.[9]

In the region of the ν_{as} PO_2^- vibrations, the strong negative band at 1251 cm^{-1} in the spectrum of **1a**, which is downshifted by only 2 cm^{-1} in the γ-$^{18}O_3$ isotopomer **1c**,[1] is shifted to 1238 cm^{-1} in the β-isotopomer **5**. A new positive band appears for **5** at 1177 cm^{-1}, and there is a marked inflection point at ∼1220 cm^{-1} which is absent in the spectrum of **1a**. These results confirm our previous interpretation of the ν_{as} PO_2^- vibrations,[1] namely that the negative 1251 cm^{-1} band arises from an alteration in the vibrational modes of the α- and β-PO_2^- groups consequent on the change from caged to free ATP, now supported by the shift to 1238 cm^{-1} in **5**. In the region around 1220 cm^{-1} a positive band for the ν_{as} mode of the α- and β-PO_2^- groups of free ATP overlaps with a negative band from the ν_{as} mode of the disappearing γ-PO_2^- group of caged ATP. The result of the overlap for the unlabeled compound **1a** is to cancel absorption in this region. For the β-isotopomer **5** these absorptions no longer fully cancel because of the downshift of the positive band to 1177 cm^{-1}.

Absorption by antisymmetric modes[1,7] of the newly formed γ-PO_3^{2-} group of ATP dominates the spectrum around 1120 cm^{-1}, and the position of the absorption envelope is not shifted by β-labeling. However, the fine structure of the band profile is significantly altered because of overlapping ν_s PO_2^- modes of caged and free ATP. As also seen in the spectrum of *aci*-nitro formation, a minimum appears at 1121 cm^{-1} due to a ν_s PO_2^- mode of **5**, shifted from its position at 1131 cm^{-1} in unlabeled compound **1a**. As described above, the negative bands at 1076 and 1059 cm^{-1} present in the difference spectrum of *aci*-nitro formation are unaffected in the β-isotopomer **5**. Shoulders remain at these positions in the end spectrum (Figure 2b) but with diminished intensity. The 1059 cm^{-1} negative band was previously assigned to a ν_s PO_2^- mode of caged ATP with a strong contribution of the γ-phosphate,[1] that is perturbed in the *aci*-nitro intermediate and absent from the final free ATP. The diminished intensity for the β-isotopomer **5** is evidently caused by a further component of the intensity in the end spectrum that shifts from ∼1070 cm^{-1} for unlabeled caged ATP **1a** to 1047 cm^{-1} for **5**. For both isotopomers the negative band intensifies at these positions as the *aci*-nitro intermediate reacts to give the final products (*cf.* Figure 1c of Ref. 1). The additional negative band at 1047 cm^{-1} evidently represents a ν_s PO_2^- mode with a large contribution from the β-phosphate, that is little perturbed by formation of the *aci*-nitro intermediate but is sensitive to unmasking of the terminal phosphate. In summary, our observations of the ν_s PO_2^- modes for caged ATP are that the high wavenumber modes are less localized on individual phosphate groups than the low wavenumber modes. These data are consistent with Takeuchi's findings for ATP itself.[7]

Finally, at frequencies below 1030 cm^{-1} there are a number of changes caused by β-labeling. This spectroscopic region involves $P_\alpha-O-P_\beta-O-P_\gamma$ vibrational modes, often coupled to ν_s modes of the PO_2^- or PO_3^{2-} groups. The intensity of the negative band at 1019 cm^{-1} in the spectrum from **1a** is reduced in the spectrum from **5**, probably because of the downshift of a negative band from this position to a region close to the inflection observed at 998 cm^{-1}. The negative band at 938 cm^{-1} is downshifted to 920 cm^{-1}. The 1019 and 938 cm^{-1} bands were previously assigned[1] to backbone C−O and P−O vibrations of caged ATP, possibly with a contribution from the nonbridging P−O vibrations, and the present data support this. Two positive bands at 989 and 917 cm^{-1} that appear on formation of free ATP are affected to differing extents by β-labeling. The former is weakly downshifted by 3 cm^{-1}, while the latter is strongly downshifted with a maximum apparently below the 900 cm^{-1} limit of our spectral range. These findings indicate that the vibrational modes corresponding to the higher frequency difference bands at 1019 and 989 cm^{-1} have only a small contribution of ν_s β-PO_2^- and $P_\beta-O-P_\gamma$ vibrations, whereas the lower frequency bands at 938 and 917 cm^{-1} have a significant contribution from these modes, in agreement with Takeuchi's original assignment.[7]

Single Wavelength Kinetic Measurements. As mentioned in the Introduction, the rate measured by time-resolved single frequency IR spectroscopy in our previous work[1] for photolytic release of ATP was unexpectedly fast (218 ± 33 s^{-1} at pH 7 and 22 °C) compared to an estimated value[3] of 50 s^{-1} under the experimental conditions. We have been concerned to examine the basis of this discrepancy.

The kinetic measurements in the earlier paper were made at frequencies (1119 and 1251 cm^{-1}) that reported directly on the rate of free ATP formation. In light of the additional information obtained from the new isotopomers in the present work, we extended these kinetic measurements to other bands, some of which have now been shown to be characteristic of the *aci*-nitro portion of the overall intermediate **2**. The new measurements were made at 10 °C, and results are shown in Table 1. Figure 3b shows a typical kinetic trace to illustrate the "instantaneous" transition from caged ATP to the *aci*-nitro intermediate **2** and subsequent slower breakdown of the latter to free ATP. At all IR frequencies studied the slow phase was monoexponential, and the measured rate constants agree well

(8) Barabás, K.; Keszthelyi, L. *Acta Biochim. Biophys. Acad. Sci. Hung.* **1984**, *19*, 305−309.

(9) Colthup, N. B.; Daly, L. H.; Wiberley, S. E. *Introduction to Infrared and Raman Spectroscopy*, 3rd ed.; Academic Press: San Diego, 1990; p 296.

Table 1. Transient Kinetics of the Photochemical Cleavage of Caged ATP[a]

wavenumber,[b] cm^{-1}	step sign[c]	exponential sign[d]	k (pH 7.0), s^{-1}	k (pH 7.9), s^{-1}
1060	negative	*e*	*e*	*e*
1119	positive	positive	53 ± 3	7.4 ± 0.4
1251	positive	negative	57 ± 2	7.5 ± 0.5
1330	positive	negative	61 ± 8	7.7 ± 0.8
1347	negative	positive	*f*	*f*
1465	positive	negative	62 ± 9	8.5 ± 1.9
1527	negative	positive	47 ± 10	9.0 ± 1.8

[a] Measurements at 10 °C; data are given as mean ± SD for $n = 4$. The rate constant k corresponds to that shown in Scheme 1. [b] Spectral resolution 20 cm^{-1} except for bands at 1330 and 1347 cm^{-1}, where spectral resolution was 10 cm^{-1}. [c] Sign of the "instantaneous" absorbance change consequent on photolytic formation of the *aci*-nitro intermediate **2**. [d] Sign of the exponential change in absorbance as the *aci*-nitro intermediate **2** decays. [e] Step change in absorbance only. [f] Absorbance change subsequent to initial step too small to determine accurately.

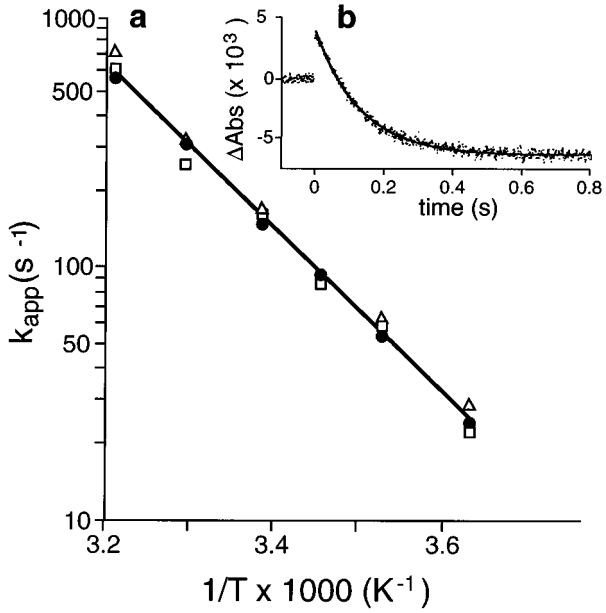

Figure 3. (a) Arrhenius plot of the kinetics of selected IR bands following flash photolysis of caged ATP, pH 7.0. ●, 1119 cm^{-1}; □, 1251 cm^{-1}; △, 1330 cm^{-1}, (b) Kinetic IR absorption recording of caged ATP photolysis measured at 1251 cm^{-1} at pH 7.9 and 10 °C. The flash artefact has been subtracted.

at the different frequencies. Further discussion of results at individual frequencies is not required, except to comment on the data for the negative 1527 cm^{-1} band, which arises from the nitro group of caged ATP that disappears upon conversion to the *aci*-nitro intermediate. We noted previously[1] that in the transition from the intermediate to the end products the intensity of the negative band diminishes and the minimum shifts by 2 to 1525 cm^{-1}. Comparable effects are seen for the ^{15}N isotopomer **1d**, where the observed shift is from 1500 to 1499 cm^{-1}. The effect is less clear for the symmetric NO_2 vibration because adjacent positive bands may distort the band profile. With this caveat, the observed absorption minimum shifts from 1347 to 1344 cm^{-1} between the intermediate and final spectra (see Figure 1 of ref 1). These observations, together with the kinetics reported here for the 1527 cm^{-1} band, confirm our previous report. Nevertheless, changes of intensity and frequency of the nitro bands as the *aci*-nitro intermediate decays are inconsistent with the mechanism shown in Scheme 1, where the nitro group is transformed within the time of the light pulse. Further investigation will be required to probe this phenomenon.

As well as these IR measurements, the transient absorbance change at 420 nm was recorded under identical conditions in the *same* experimental cell (see Experimental Section for details) and showed the expected instantaneous increase in absorbance upon flash irradiation, followed by an exponential decay at 52 ± 3 s^{-1} (pH 7.0, 10 °C), that is concordant with the IR measurements (Table 1). Thus the data conclusively equate the decay rates of the *aci*-nitro intermediate **2** measured by different techniques with the rate of release of the ATP product. Nevertheless we were concerned to resolve the discrepancy between our earlier IR measurement[1] of the ATP release rate (mean 218 s^{-1} at pH 7.0, 22 °C) and the values now reported. As one approach we used transient UV−visible spectroscopy in a larger optical cell[2] to obtain a reference decay rate of the *aci*-nitro intermediate **2** for comparison with the IR kinetic measurements. Because of the longer optical path length in this UV-visible experiment, it was necessary to use a solution with a much lower concentration of caged ATP. The solution had a sufficiently large volume to ensure accurate pH determination and was supplemented with ADP to mimic the ionic strength contribution made in the IR solutions by caged ATP. The measured rate of *aci*-nitro decay had a mean value of 92 s^{-1} at pH 7.0 and 20 °C, i.e., approximately 2.4-fold slower than the rate previously determined[1] by IR measurements under similar conditions. We believe the likely source of the discrepancy is a variation of pH: the difficulties for accurate pH control when mixing concentrated solutions of caged ATP and buffers in the small (1−2 μL) volumes used for the IR measurements are illustrated by the systematic difference between the rates measured in our earlier and present studies. Furthermore the buffering of the IR solutions may be insufficient to compensate for the protons released by photolysis of the high concentration of caged ATP. Thus while the IR measurements are able to provide an excellent linkage of *aci*-nitro decay and product release rates, for accurate estimation of the *aci*-nitro decay rate it is desirable to work in dilute, well buffered solutions.

In the final part of this section, we determined the temperature dependence of the decay rate of the *aci*-nitro intermediate at pH 7.0 over the range 2−40 °C, using measurements at three IR frequencies (1119, 1251, and 1330 cm^{-1}), of which the first and last are specific for release of ATP and for *aci*-nitro decay respectively, while the middle value reports a combination of these. Measurements at each frequency showed identical temperature dependence, and the results are shown as an Arrhenius plot (Figure 3a), from which the measured activation energy is 62 ± 2 kJ mol^{-1}. This value agrees with work by Barabás and Keszthelyi,[8] who reported an activation energy in the range 52−67 kJ mol^{-1} for data from UV measurements in 10 mM buffer over the pH range 6−8.

Characterization of Byproducts from the 1-(2-Nitrophenyl)ethyl Group at pD 6.0. (a) In the Absence of a Thiol. For reasons outlined in section (b) below, experiments to characterize the photolysis products that arise from the 1-(2-nitrophenyl)ethyl group were performed under mildly acidic conditions at 35 °C. These experiments were performed in D_2O buffer solutions in order that the spectral region 1550−1700 cm^{-1} was not obscured by solvent absorption: changing between H_2O and D_2O did not otherwise affect the spectra. Spectroscopic features were essentially identical over the pH range 6.0−7.5, but at the lower pH the time courses of their evolution were more accessible to observation. Figure 4a shows difference spectra of photolysis of caged ATP **1a** performed in the absence of a thiol. Acquisition of spectra began 4 ms after the photolysis flash, by which time at pH 6 and 35 °C decay of

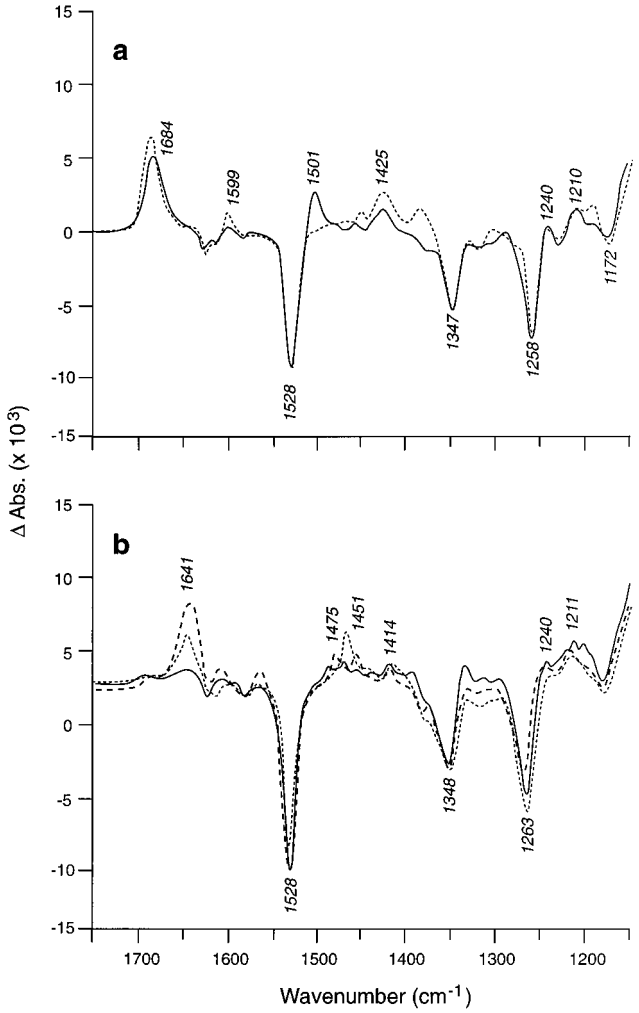

Figure 4. (a) Infrared difference spectra of caged ATP photolysis in the absence of dithiothreitol (DTT) at pD 6.0, 35 °C. Spectra were obtained 4−60 ms (solid line) and 1.3−24 s (dotted line) after the photolysis flash. Labels refer to peaks in the solid line spectrum. (b) Infrared difference spectra of caged ATP photolysis in the presence of 200 mM DTT at pD 6.0, 35 °C. Spectra were obtained 4−60 ms (solid line), 0.3−3.6 s (dashed line), and 120−140 s (dotted line) after the photolysis flash. Labels refer to peaks in the dashed line spectrum.

the *aci*-nitro intermediate is >99% complete. Thus the spectra represent only reactions of the 2-nitrosoacetophenone byproduct **3** and its *cis*- and *trans*-dimers. They were acquired principally as part of our investigation of the end product formed in the presence of a thiol [see section (b) below], but they are discussed briefly here as they also reveal features of the chemistry of 2-nitrosoacetophenone. As would be expected, there were no significant changes in phosphate modes as ATP release is already complete. Therefore this spectral region is omitted from Figure 4.

The spectra in Figure 4a were acquired in the time frames 4−60 ms and 1−3.6 s after the photolysis flash, and the changes between the two are a consequence of dimerization of the nitroso group of **3**. The first spectrum shows positive bands at 1501 and 1425 cm^{-1} (shifted to 1485 and 1417 cm^{-1} respectively by ^{15}N substitution). The band at 1501 cm^{-1}, characteristic for the nitroso monomer,[10] decayed with an estimated 0.17 s half-time as the nitroso dimer formed. The carbonyl absorption moves from 1684 to 1686 cm^{-1} as the dimerization proceeds (1647 and 1649 cm^{-1}, respectively upon ^{13}C substitution). The spectrum after dimerization has bands at 1425 and 1385 cm^{-1} (shifted to 1393 and 1348 cm^{-1} by ^{15}N substitution) that are close to positions of 1409 and 1389−1397 cm^{-1} reported for *cis*-nitroso dimers.[10] The disappearance of the monomer band at 1425 cm^{-1} and its replacement by the dimer band at the same position could only be observed in the ^{15}N compound **1d**, for which the two bands were shifted to different extents. Upon longer incubation at 35 °C (spectrum acquired at 42−62 s; not shown) a positive band appears at 1269 cm^{-1} (1243 cm^{-1} with ^{15}N substitution), close to the position (~1257 cm^{-1}) at which *trans*-nitroso dimers absorb.[10] The growth of the 1269 cm^{-1} band was accompanied by a decrease in the absorption bands of the *cis*-dimer. Evidently the chemistry of the photolysis byproduct at neutral or weakly acidic pH and in the absence of a thiol is essentially that expected[11,12] for the known byproduct,[2] 2-nitrosoacetophenone **3**. At pH 8.5 none of the bands characteristic of the nitrosoketone was observed, except for a carbonyl absorption at 1686 cm^{-1}. Evidently other reactions supervene at higher pH, but we have not pursued this matter as it is of little relevance to uses of caged compounds in biology.

(b) In the Presence of a Thiol. The most striking differences between the IR spectra recorded after photolysis at 35 °C with and without dithiothreitol (DTT) present are in the region 1600−1700 cm^{-1} (compare Figure 4a,b). In the presence of DTT the first spectrum, recorded 4−60 ms after the photolysis flash, shows almost no absorption in this region, but in the second spectrum, recorded 0.3−3.6 s after the flash, a strong band appears at 1641 cm^{-1}. The intensity of this band diminishes upon further incubation, and its maximum shifts to 1645 cm^{-1}, with a shoulder at higher frequency (third spectrum, at 120−140 s). The intensity of the negative band at 1528 cm^{-1} in the third spectrum is diminished by the appearance of an overlapping positive band (see below). These changes between the second and third spectra were paralleled in the region 1450−1480 cm^{-1}, where two medium intensity bands at 1451 and 1475 cm^{-1} in the second spectrum were replaced by a single stronger band at 1466 cm^{-1} in the final spectrum. The bands at 1475 (second spectrum) and 1466 cm^{-1} (third spectrum) are downshifted by 2 and 3 cm^{-1}, respectively, upon ^{15}N substitution (isotopomer **1d**). The most pronounced effect of ^{13}C substitution (isotopomer **1e**) is a downshift of 32 cm^{-1} for the band at 1641 cm^{-1} in the second spectrum. In the final spectrum the bands at 1645 and 1466 cm^{-1} are downshifted by 6 and 5 cm^{-1}, respectively.

To gain further information about this reaction sequence, we monitored the UV spectral changes which took place when 2-nitrosoacetophenone was treated with excess DTT in a 1 cm path length cuvette, where times to add reagents and record spectra were each 20−30 s. Therefore the first intermediate seen by IR spectroscopy is missed in these experiments. The results are given in Figure 5a, which shows that the spectrum of the nitrosoketone is promptly converted to a much less intense spectrum (λ_{max} 343 nm) upon addition of the thiol. Upon longer incubation (*ca.* 1 h at pH 7, 35 °C for completion) this spectrum was transformed to a final spectrum with a maximum at 316 nm and several smaller peaks between 265 and 280 nm. Single wavelength kinetic monitoring at 316 nm under the same conditions (Figure 5b) showed a half-time of 9 min for the development of the final spectrum. The rate of this absorbance change was unaffected by doubling the thiol concentration but increased by an order of magnitude at pH 6.0 (data not shown). We note that at the <1 mM concentrations used here and in related kinetic experiments below, the nitrosoketone is entirely

(10) Reference 9, p 353.

(11) Azoulay, M.; Fischer, E. *J. Chem. Soc., Perkin Trans. 2* **1982**, 637−642.

(12) Zuman, P.; Shah, B. *Chem. Rev.* **1994**, *94*, 1621−1641 and references therein.

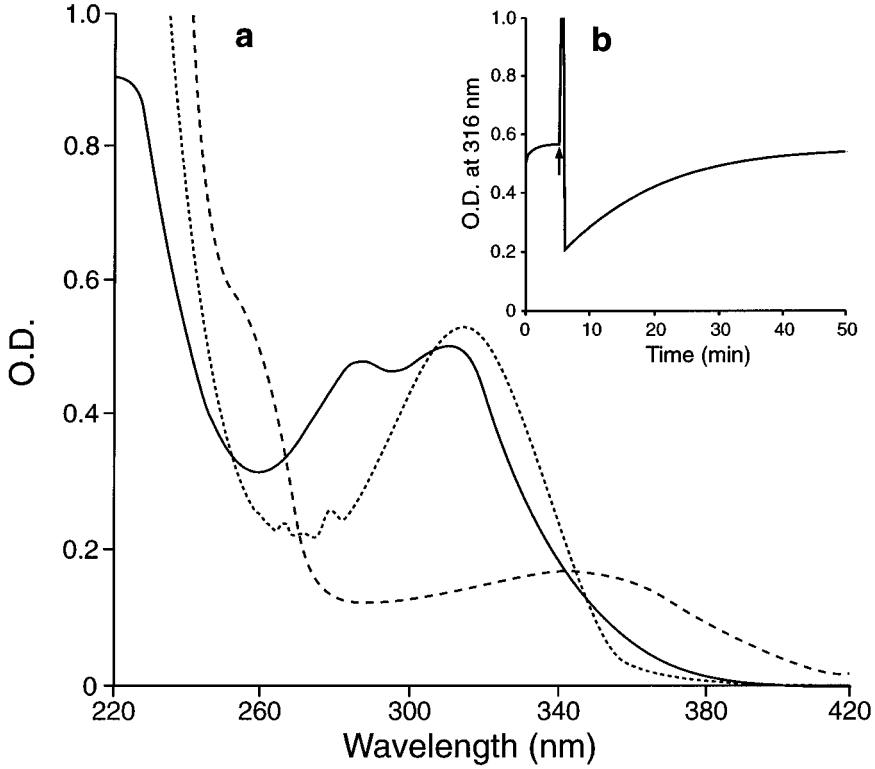

Figure 5. (a) Ultraviolet spectra showing the reaction of 2-nitrosoacetophenone (0.118 mM) with DTT (5 mM) at pH 7.0, 35 °C. Solid line, 2-nitrosoacetophenone; dashed line, 2-nitrosoacetophenone within 30 s after addition of excess DTT; dotted line, spectrum after 1 h. (b) Time-dependent absorbance at 316 nm. The arrow shows the time of mixing excess DTT with the 2-nitrosoacetophenone solution.

in the monomeric form, as shown by ^{1}H NMR spectra run at varying concentrations (see Experimental Section). The dimer is undetectable at 2 mM concentration in either $CDCl_3$ or CD_3OD solution. Also the UV spectrum (Figure 5a) shows the double peak typical of monomeric aromatic nitroso compounds.[11] Therefore the spectral changes seen here and in previous[2] kinetic experiments are not influenced by the monomer−dimer equilibrium of 2-nitrosoacetophenone.

Previous kinetic work[2] based on absorbance measurements at 380 nm had found two steps in the reaction of DTT with 2-nitrosoacetophenone. The final, slow step identified in the present work was beyond the time scale of the earlier experiments. At pH 7.0, 21 °C the first process had a second-order rate constant of 3.5×10^3 M^{-1} s^{-1}. The second process was independent of DTT concentration, with an observed first-order rate constant of 45 s^{-1}. The product of the second step had a UV spectrum with a maximum at 373 nm (measured in ethanol by difference spectroscopy against the starting nitrosoketone).[2] When the experiment of Figure 5a was repeated in ethanol solution, a similar absorbance maximum was observed at 380 nm instead of the 343 nm value found in aqueous solution.

The results of the previous kinetic measurements and the present IR and UV spectroscopic studies have been interpreted for the case where DTT is the thiol in Scheme 2. The sequence is initiated by nucleophilic addition of a thiolate anion to the nitroso group of **3** to give the intermediate **6**, which is inferred to exist predominantly in its cyclic form (see below). By contrast, the product of the second step appears to exist as a mixture of the closed and open forms **7** and **8**, respectively. The long-wavelength absorption band in the intermediate UV spectrum at 343 nm is unlikely to arise from **7** but would be consistent with the presence of a proportion of the open-chain form **8** [*cf.* 2-aminoacetophenone[13] has λ_{max}(EtOH) 359 nm].

Scheme 2

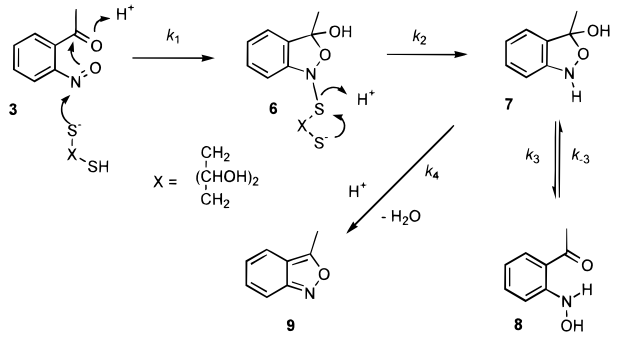

Furthermore, the band at 1641 cm^{-1} in the IR spectrum at 0.3−3.6 s (Figure 4b, dashed line) is consistent with an internally hydrogen bonded carbonyl as would be expected in **8** [*cf.* 1636 cm^{-1} for 2-aminoacetophenone as a saturated solution in D_2O (data not shown)]. The initial steps of Scheme 2 are in agreement with previous studies of thiol reactions with aromatic nitroso compounds[12] and in particular with a report that 4-nitrosoacetophenone is reduced by thiols to the corresponding hydroxylamine.[14]

The overall transition from **6** to **7**/**8** involves an irreversible reduction of the N−S bond followed by a ring-chain tautomerism, and we wished to establish which of these steps corresponded to the 45 s^{-1} process seen previously.[2] The best studied analogy for the intramolecular reduction of **6** is from the extensive studies by Whitesides *et al.* of thiol-disulfide interchange reactions: with DTT the second (intramolecular) step to cleave the mixed disulfide is faster than the initial interchange[15a] because of the high effective concentration[15b] of the intramolecular thiol group of DTT. Thus the reduction of

(13) Weast, R. C. *Handbook of Chemistry and Physics, 50th ed.;* Chemical Rubber Co.: Cleveland, OH, 1969; p C-93.

(14) Diepold, C. H.; Eyer, P.; Kampffmeyer, H.; Reinhardt, K. *Adv. Exp. Med. Biol.* **1982**, *136B*, 1173−1181.

Table 2. Rate Constants for Ring-Chain Tautomerism of 2-Hydroxylaminoacetophenone **7**/**8** at 15 °C

pH	k_3, s^{-1}	k_{-3}, s^{-1}
7.5	1.32	0.33
8.0	4.5	1.15
8.5	15.0	4.7

[a] See Experimental Section for details of solution conditions. [b] For definitions of k_3 and k_{-3} see Scheme 2.

6 might be expected to be a rapid step. By contrast, rates of ring-chain tautomerism within one set of related compounds can be modulated by substituent effects to span at least three orders of magnitude[16] and prediction of the **7** ⇌ **8** interchange rates was uncertain. We measured these two rate constants using a saturation-transfer NMR technique[17] for solutions of the ring-chain tautomers **7** and **8** prepared by treating a choloroform/methanol solution of 2-nitrosoacetophenone **3** with aqueous solutions of DTT buffered over the pH range 7.5−8.5. The spectra showed two singlets with an intensity ratio of ∼1:4 at δ 1.83 and 2.63, respectively. The latter overlapped with a multiplet in the range δ 2.6−2.75 arising from DTT but could readily be deconvoluted (see Experimental Section). Continuous irradiation of the upfield singlet caused a marked decrease in the peak height of the singlet at δ 2.63, thereby confirming that the two signals arose from species in chemical exchange. The signal at δ 1.83 corresponds to the cyclic tautomer **7** and the signal at δ 2.63 to the open form **8**. Details of the saturation-transfer experiments are given in the Experimental Section and the derived rate constants for ring opening (k_3) and closing (k_{-3}) are given in Table 2. Figure 6a shows data for the measurements at pH 8.0.

Assuming that Scheme 2 correctly interprets the overall process, the observed rate of the 380 nm transient, k_{obs}, is given by ($k_3 + k_{-3}$). Extrapolation from the data of Table 2 suggests that at pH 7.0 and 15 °C, k_{obs} would be ∼0.56 s^{-1}, i.e., much slower than the value of 45 s^{-1} measured at pH 7.0, 21 °C.[2] Since the NMR data were obtained under different conditions of solvent, temperature, and ionic strength to the original flash photolysis measurements, we repeated the latter under conditions identical to one set of the NMR experiments (pH 8.0, 15 °C). 2-Nitrosoacetophenone was generated rapidly by flash photolysis of 1-(2-nitrophenyl)ethyl phosphate (caged P_i) for which the decay of the *aci*-nitro anion has a half-time ∼0.1 ms under these conditions.[2] The observed rate constant of the 380 nm transient was 14 s^{-1} in protiated solvent (H_2O-CH_3OH) and 8.6 s^{-1} in deuterated solvent (D_2O-CH_3OD; Figure 6b). These rate constants were unaffected by changing the DTT concentration from 100 to 300 mM, and the value in the deuterated solvent agrees well with that of 5.65 s^{-1} measured by NMR. These data provide strong evidence that the rate-determining step of the 380 nm transient is the ring to chain tautomerism **7** → **8**, i.e., $k_2 \gg (k_3 + k_{-3})$. There are insufficient data to determine whether the approximately 2-fold decrease in rate in the deuterated solvent arises from small pH discrepancies between the two solutions or from a kinetic isotope effect.

With a monovalent thiol, the previous analogy with thiol/disulfide interchange reactions[15] suggests that reduction of the analogue of **6** to give **7** may be much slower. The possibility

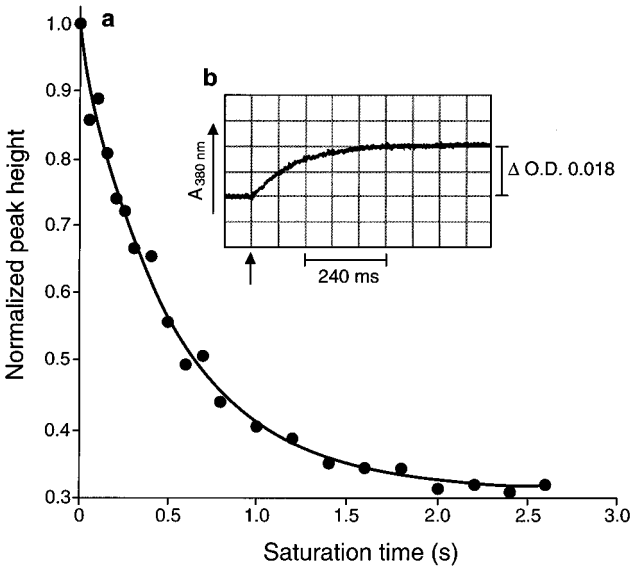

Figure 6. (a) Height of the NMR signal at δ 2.63 as a function of the saturation time at δ 1.83 for a pH 8.0 solution of 2-hydroxylaminoacetophenone **7**/**8** at 15 °C (see Experimental Section for details of solution composition). Peak heights are normalized to the height of the signal without irradiation. (b) Absorbance transient at 380 nm following flash photolysis of 1-(2-nitrophenyl)ethyl phosphate in the presence of 100 mM DTT at pH 8.0, 15 °C (deuterated solvent, see Experimental Section for details of solution composition). The arrow on the abscissa marks the time of the laser flash. The optical path length was 4 mm.

of consecutive reactions (analogous to **6** → **7** ⇌ **8**) with comparable rates for each step may explain the complex thiol dependence for the rate of formation of **8** when a monofunctional thiol was used.[2] For DTT (Scheme 2) the initial adduct **6** appears not to be present in significant concentration. Thus the IR spectrum recorded in the 4−60 ms time frame principally represents the reduced compound **7**. Subsequent establishment of the **7** ⇌ **8** equilibrium is represented in the spectrum acquired at 0.3−3.6 s. The initial formation of **7** implies that its precursor **6** is also in the cyclic form shown and it is of interest why **6** exists in the cyclic form, whereas for **7**/**8** the equilibrium favors the open form. The open form **8** is stabilized by its strong internal hydrogen bond. By contrast, in an open tautomer of **6**, there would be steric interactions between the substituents on the nitrogen and the *o*-acetyl group. These interactions would be relieved by cyclization.

The final step of Scheme 2 proposes an acid-catalyzed dehydration of **7**/**8** to generate 3-methylanthranil **9** (3-methyl-2,1-benzisoxazole) as the end product responsible for the IR bands at 1645 and 1466 cm^{-1} (Figure 4b) and the UV absorption at 316 nm (Figure 5a). The final UV spectrum closely matches that of 3-methylanthranil,[18] and the absorbance at 316 nm corresponds to its formation in 74% yield. A strong band at 1521 cm^{-1} in the IR spectrum of 3-methylanthranil (see Experimental Section) is obscured by the negative band at 1528 cm^{-1} in the final difference spectrum arising from photolysis of the unlabeled compound **1a** but is observable at 1525 cm^{-1} in the corresponding spectrum from the ^{15}N isotopomer **1d** where the negative band is strongly downshifted. The small isotopic shifts observed in the IR spectrum of 3-methylanthranil (see above) indicate that the bands do not arise from localized vibrational modes. By comparison, the IR spectrum of

(15) (a) Whitesides, G. M.; Lilburb, J. E.; Szajewski, R. P. *J. Org. Chem.* **1977**, *42*, 332−338. (b) Burns, J. A.; Whitesides, G. M. *J. Am. Chem. Soc.* **1990**, *112*, 6296−6303.

(16) Valters, R. E.; Flitsch, W. *Ring-Chain Tautomerism*; Plenum Press: New York, 1985; Chapter 2.

(17) Cayley, P. J.; Albrand, J. P.; Feeney, J.; Roberts, G. C. K.; Piper, E. A.; Burgen, A. S. V. *Biochemistry* **1979**, *18*, 3886−3895. Hyde, E. I.; Birdsall, B.; Roberts, G. C. K.; Feeney, J.; Burgen, A. S. V. *Biochemistry* **1980**, *19*, 3738−3746.

(18) Yates, P.; Hand, E. S. *J. Am. Chem. Soc.* **1969**, *91*, 4749−4760.

[$^{13}C_1$]benzene has been analyzed in detail and shows similarly small shifts for almost all bands.[19]

The data presented above in support of Scheme 2 are all spectroscopic, and we wished to obtain some additional chemical evidence. To confirm the intermediacy of the hydroxylamine **8**, a solution of 2-nitrosoacetophenone in chloroform (with added triethylamine to maintain a basic environment and suppress dehydration to the anthranil) was treated with excess DTT. The major product isolated was the azoxybenzene **10**, formation of which provides evidence for the presence of hydroxylamine **8**, since it would be generated by condensation of **8** with the starting nitrosoketone. The result also suggests that the reaction kinetics in chloroform differ from those in aqueous solution, since in the latter case the nitrosoketone would mostly be consumed by the first reaction with thiol before a significant concentration of the hydroxylamine could be formed.

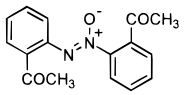

10

To confirm the formation of 3-methylanthranil, caged ATP solutions at pH 7 that contained excess DTT were photolyzed using a single 50 ns pulse of 347 nm light from a frequency-doubled ruby laser,[2,20] and the products were analyzed quantitatively by reverse-phase and anion-exchange HPLC. Single flash photolysis of 9.8 mM caged ATP released 1.0 mM ATP (anion-exchange HPLC). Reverse-phase HPLC showed a major hydrophobic component which coeluted with authentic 3-methylanthranil and corresponded to formation of the compound at a concentration of 0.74 mM, i.e., 74% of the released ATP concentration. Several unidentified minor peaks presumably account for the remaining materials balance. In keeping with the time course of formation of 3-methylanthranil shown in Figure 5b, it was notable that the height of the HPLC peak corresponding to this compound did not stabilize until the photolyzed solution had been allowed to stand for ~1 h after irradiation. Chromatograms run at earlier times showed a peak with a shorter retention time, that disappeared as the 3-methylanthranil peak stabilized. This peak was present in chromatograms run immediately after mixing 2-nitrosoacetophenone with DTT and evidently corresponds to the equilibrium mixture of **7** and **8**. Reduction of 2-nitrosoacetophenone to 3-methylanthranil has previously been reported by electrochemistry under acidic conditions,[21] with triphenylphosphine[22] and with bisulfite.[23] Nevertheless, on the time scale of most biological experiments that use caged compounds, the major byproduct species present must be the tautomeric forms **7** and **8** of 2-hydroxylaminoacetophenone, although when a monofunctional thiol is used significant concentrations of the initial thiol adduct with 2-nitrosoacetophenone may also be present.

Conclusion. Photochemical rearrangements and photochromism of *ortho*-substituted nitro compounds have been of fundamental interest for almost 100 years.[24] In particular, the photocleavage of *o*-nitrobenzyl derivatives has played a pivotal role in the development of caged compounds for rapid release of biological effectors. The results presented above demonstrate the utility of time-resolved infrared spectroscopy as a tool for mechanistic and product investigations of the photolysis of caged compounds. Provided that the necessary stable isotopomers of a compound under study can be synthesized to enable definitive identification of relevant IR bands, the method is capable of unequivocal and direct determination of the rate of product release from its caged precursor. Notably it should enable detailed investigation of caged compounds that show biphasic decay of putative *aci*-nitro anion intermediates when observed by transient UV spectroscopy.[25] The capacity of the method to aid identification of photolysis products has also been demonstrated in this work and in a further recent application where we have confirmed an unexpected decarboxylation which occurs during photolysis of sulfonamide-protected derivatives of amino acids.[26]

Experimental Procedures

Materials. Caged ATP **1a** was prepared by esterification of ATP with 1-(2-nitrophenyl)diazoethane as previously described,[2] and the $\beta,\beta\gamma$-$^{18}O_3$ analogue **5** was prepared similarly from [$\beta,\beta\gamma$-$^{18}O_3$]ATP,[27] for which the overall isotopic enrichment was 90%. The ^{15}N and ^{13}C analogues of caged ATP (**1d**, **1e**) and of caged methyl phosphate (**4b**, **4c**) were prepared as described,[28] and [^{18}O]caged methyl phosphate **4d** was prepared similarly from [^{18}O]caged phosphate.[29] For FTIR measurements at pH 8.5, solutions contained the caged compound (85−120 mM) in *N*,*N*-bis(2-hydroxyethyl)glycine−KOH (Bicine) buffer (200 mM, pH 8.5). For measurements at pD 6.0 to study the byproducts, aliquots (1 μL each) of solutions in H_2O of the caged compound (85−120 mM) and 2-(*N*-morpholino)ethanesulfonic acid−KOH (MES) buffer (200 mM, pH 6.0) plus DTT (200 mM) where required were evaporated on the IR window under a nitrogen stream and reconstituted in D_2O (1 μL). For the single-frequency kinetic measurements, solutions contained caged ATP (90 mM) in *N*-(2-acetamido)iminodiacetic acid−KOH (ADA) buffer (800 mM, pH 7.0) or Bicine buffer (800 mM, pH 7.9). Silica gel (Merck 9385) was used for flash chromatography.

Spectroscopy. Details of the FT and dispersive IR spectrometers have been given previously.[1] For measurement of transient signals at 420 nm in the same cell as used for the FTIR and single-frequency experiments, the sample was placed in a spectrometer fitted with the same xenon flash tube as used in the IR spectrometers, a monochromator (H20, Jobin Yvon, Longjumeau, France), and a photodiode detector and preamplifier built in W.M.'s laboratory. The sample composition was the same as for the IR measurements. Separate measurement of the UV transient with a dilute solution of caged ATP was performed as previously described,[2] for a solution containing caged ATP (0.5 mM), ADP (90 mM), and K-ADA buffer (800 mM, pH 7.0).

2-Nitrosoacetophenone 3. This compound was prepared as described.[30] The ^1H NMR spectrum (2 mM in $CDCl_3$) had δ (400 MHz) 2.75 (s, 3H), 7.00 (d, 1H), 7.60 (t, 1H,), 7.71 (d, 1H) and 7.78 (t, 1H). At 100 mM in $CDCl_3$ all these signals were still present but were complemented by a further set of signals from the dimer at δ 2.68 (s, 6H), 7.66 (t, 3H), 7.78 (t, 3H), 7.90 (d, 1H), and 7.91 (d, 1H). The intensity of the latter set of signals was reduced in a spectrum at 15 mM concentration (1:11 molar ratio of dimer:monomer) compared to a spectrum at 100 mM (1:3 dimer:monomer).

(19) Brodersen, S.; Christoffersen, J.; Bak, B.; Nielsen, J. T. *Spectrochim. Acta* **1965**, *21*, 2077−2084.

(20) McCray, J. A.; Herbette, L.; Kihara, T.; Trentham, D. R. *Proc. Natl. Acad. Sci. U.S.A.* **1980**, *77*, 7237−7241.

(21) Le Guyader, M. *C. R. Seances Acad. Sci., Ser. C* **1966**, *262*, 1383−1386.

(22) Shabarov, Y. S.; Mochalov, S. S.; Fedotov, A. N.; Kalashnikov, V. V. *Khim. Geterotsikl. Soedin.* **1974**, *9*, 1195−1197.

(23) Fedotov, A. N.; Mochalov, S. S.; Shabarov, Y. S. *Zh. Prikl. Khim.* **1977**, *50*, 1775−1777.

(24) Wettermark, G.; Black, E.; Dogliotti, L. *Photochem. Photobiol.* **1965**, *4*, 229−239. DeMayo, P.; Reid, S. T. *Quart. Rev. (London)* **1961**, *15*, 393−417. Morrison, H.; Migdalof, B. H. *J. Am. Chem. Soc.* **1965**, *30*, 3996.

(25) Corrie, J. E. T. *J. Chem. Soc., Perkin Trans. 1* **1993**, 2161−2166. Peng, L; Goeldner, M. *J. Org. Chem.* **1996**, *61*, 185−191. Ellis-Davies, G. C. R.; Kaplan, J. H.; Barsotti, R. J. *Biophys. J.* **1996**, *70*, 1006−1016.

(26) Corrie, J. E. T.; Papageorgiou, G. *J. Chem. Soc., Perkin Trans. 1* **1996**, 1583−1592.

(27) Cohn, M.; Hu, A. *J. Am. Chem. Soc.* **1980**, *102*, 913−916.

(28) Corrie, J. E. T. *J. Labelled Compd. Radiopharm.* **1996**, *38*, 403−410.

(29) Corrie, J. E. T.; Reid, G. P. *J. Labelled Compd. Radiopharm.* **1995**, *36*, 289−300.

(30) Shabarov, Y. S.; Mochalov, S. S.; Stepanova, I. P. *Dokl. Akad. Nauk SSSR* **1969**, *189*, 1028−1030.

3-Methylanthranil 9. Prepared as described[22] by reduction of 2-nitrosoacetophenone with triphenylphosphine to give a colorless oil: bp (Kugelrohr oven temperature) 190 °C (2 mmHg); UV [25 mM Na phosphate, pH 7.0−EtOH (9:1)] λ_{max} nm (ϵ, M^{-1} cm^{-1}) 257 (1270), 261 (1360), 266 (1640), 271 (1500), 278 (1900), 316 (6100); IR (film) 1643 (vs), 1566 (m), 1521 (s), 1463 (s), 1441 (m), 1401 (m), 1377 (w), 1284 (w), 1220 (m), 1163 (m), 1144 (m), 1081 (w), 1032 (w), 987 (m) cm^{-1}; ^{1}H NMR ($CDCl_3$, 90 MHz) δ 2.78 (s, 3H), 6.82−7.57 (m, 4H).

2,2′-Diacetylazoxybenzene 10. Dithiothreitol (75 mg, 5 mmol) was added in one portion to a stirred solution of 2-nitrosoacetophenone (250 mg, 1.67 mmol) and triethylamine (505 mg, 5 mmol) in chloroform (50 mL). After 10 min, the solution was washed with water, dried, and concentrated. The residue was flash chromatographed [EtOAc−hexanes (20:80)] to give **10**: mp 115−116.5 °C (from EtOAc−hexanes); UV (EtOH) λ_{max} nm (ϵ M^{-1} cm^{-1}) 243sh (13 100), 313 (5700); IR (Nujol) 1690, 1685, 1595, 1265, 765 cm^{-1}; ^{1}H NMR ($CDCl_3$) δ 2.56 (s, 3H), 2.59 (s, 3H), 7.27−7.83 (m, 7H), 8.04−8.19 (m, 1H). Anal. Calcd for $C_{16}H_{14}N_2O_3$: C, 68.07; H, 5.00; N, 9.92. Found: C, 67.86; H, 4.95; N, 9.89.

Reaction of 2-Nitrosoacetophenone with DTT Studied by UV Spectroscopy. A solution of 2-nitrosoacetophenone (1 mL, 1.18×10^{-4} M) in 10 mM Na phosphate, pH 7.0−EtOH (9:1) was equilibrated at 35 °C in a 1 cm path length quartz cuvette placed in a Beckman DU70 spectrophotometer, and the absorbance spectrum was recorded. An aliquot (25 μL) of a solution of DTT (200 mM) in 10 mM Na phosphate, pH 7.0 was added, and the spectrum was recorded within 30 s. Incubation was continued for 1 h, and a further spectrum was recorded. In a subsequent experiment, this protocol was repeated, but absorbance at 316 nm was monitored continuously.

Ring-Chain Tautomerism of 2-Hydroxylaminoacetophenone. Solutions of 20 mM Tricine were adjusted with 1 M NaOH to pH values of 7.5, 8.0, and 8.5, lyophilized, and redissolved in D_2O to restore the original concentration. Each solution was made to 5 mM with DTT. Aliquots (30 μL) of a $CDCl_3$ solution of 2-nitrosoacetophenone (100 mM) were diluted with CD_3OD (470 μL), and these solutions were mixed with aliquots (500 μL) of the buffered DTT solutions. Each solution for NMR was prepared immediately before the measurements began and equilibrated at 15 °C in the probe of a Bruker AM 400WB NMR spectrometer. Spectral data were processed and analyzed using the Varian VNMR 5.1 software package[31] running on an Axil Sparcstation 10/40 clone. The experimental protocol was designed to correct for the slow dehydration of the **7**/**8** mixture to 3-methylanthranil. Thus for each sample a series of interleaved FIDs was collected with irradiation of the signal at δ 1.83 for each of 20 saturation times in the range 0.1−2.6 s, applied in randomized order. Two further FIDs were interleaved, again in randomized order, either with continuous saturation or with the decoupler gated off, corresponding to infinite and zero saturation times, respectively. The sequence was repeated to give a total of eight transients for each saturation time. A delay $>5 \times T_1$ was inserted prior to each saturation pulse to eliminate fast-pulsing artifacts. T_1 was estimated using the inversion recovery method.[32] Plots of the measured line height for the signal at δ 2.63 versus saturation time were fitted to a single exponential using the Kaleidagraph software[33] running on an Apple PowerMacintosh, and the lifetime of **8** was calculated as previously described.[17]

The relative concentrations of **7** and **8** were estimated from the areas of Lorentzian-shaped peaks fitted to the signals at δ 1.83 and 2.63 using the line deconvolution methodology within VNMR 5.1. The lifetime of **7** and the corresponding rate constants were calculated from these data.[17]

To study the formation of 2-hydroxylaminoacetophenone by transient absorption spectroscopy at 380 nm following flash photolysis (Figure 6b), a solution containing 1-(2-nitrophenyl)ethyl phosphate[29] (2 mM), DTT (200 or 600 mM), and Tricine (20 mM) was diluted with an equal volume of methanol. For corresponding experiments in deuterated solvent, the buffer and DTT were exchanged with D_2O as described above, and the final D_2O solution was diluted with CH_3OD. Solutions were equilibrated at 15 °C and photolyzed with a 1 μs pulse of 320 nm laser light, and the absorption at 380 nm was recorded as previously described.[2]

Identification and Quantification of 3-Methylanthranil from Photolysis of Caged ATP in the Presence of DTT. An aliquot (20 μL) of a solution of caged ATP **1a** (9.8 mM) and DTT (20 mM) in Na phosphate buffer (25 mM, pH 7.0) was placed in a 25 μL cell at 19 °C and irradiated with a single 50 ns pulse of 347 nm light from a frequency-doubled ruby laser (Laser Applications Inc., Winter Park, FL). The average energy of the light flash was 93 mJ (range 70−110 mJ). Six irradiated aliquots were combined and analyzed by anion exchange and reverse-phase HPLC. HPLC mobile phase flow rates were 1.5 mL min^{-1}, and compositions were as follows: for anion exchange [Whatman Partisphere SAX column, Cat. no. 4621-0505; detection at 254 nm, 0.25 M $(NH_4)H_2PO_4$ (adjusted to pH 5.5 with 2 M NaOH) plus 13% MeOH (v/v)]; for reverse-phase [Merck Lichrosphere RP8 column, Cat. No. 50832; detection at 313 nm, 25 mM NaH_2PO_4 (adjusted to pH 6.5 with 2 M NaOH)−MeOH (3:2 v/v)]. Retention times (min) were as follows: (anion exchange), caged ATP 3.4, ATP 14.0; (reverse-phase), 3-methylanthranil 11.7. The different analytes caused no mutual interference on their respective columns.

Concentrations of ATP and 3-methylanthranil in the photolyzed solution were determined by comparison of chromatographic peak heights with those from reference solutions of the authentic compounds. In the reverse-phase chromatogram of the photolyzed solutions, minor peaks with retention times 3.6, 7.0, and 8.4 min were present in addition to the main peak for 3-methylanthranil. The first of these peaks disappeared as the peak for 3-methylanthranil stabilized.

Acknowledgment. We are grateful to Dr. M. R. Webb for the gift of [β,$\beta\gamma$-$^{18}O_3$]ATP. We thank the MRC Biomedical NMR Centre for access to facilities, Dr. J. Feeney for valuable discussions on the saturation-transfer experiment, and Dr. V. R. N. Munasinghe for help with NMR spectroscopy. This work was supported by an ARC grant from the Deutscher Akademischer Austauschdienst and the British Council, and by a fellowship from the Ciba-Geigy Foundation (to Y.M.).

JA964430U

(31) VNMR Version 5.1; Varian Associates, Palo Alto, CA, 1995.

(32) Harris, R. K. *Nuclear Magnetic Resonance Spectroscopy*; Pitman, London 1983; p 81.

(33) Kaleidagraph; Synergy Software, Reading, PA, 1994.